Spherical Transducers for High Intensity Focused Ultrasound Thermal Therapy

Ashraf Talaat Ibrahim
Elec.,Eng.,Dept., Faculty of engineering, Alexandria University, Alexandria Egypt.
ashraftalaat@yahoo.com

Abstract

High intensity focused ultrasound thermal therapy can be used to destroy deep seated tumors non-invasively. Due to the strong focusing and simplicity, highly focused spherical transducers have been widely adopted for HIFU applications. However, highly focused spherical transducers are not optimal because the thermal lesions they generate are very small, leading to impractically long treatment times. Moderately focused spherical transducer can produce larger thermal lesions compared to highly focused transducers. However, due to the weak focusing, more heat may be deposited in surrounding normal tissues. Although some encouraging results have been reported, it is difficult to quantitatively evaluate the ability of moderately focused spherical transducer to reduce the treatment times for large tissue volumes. A theoretical study of comparing treatment times required for highly and moderately focused spherical transducers to treat the same target under identical treatment conditions is presented here. A 3-D ultrasound thermal model was developed to calculate thermal dose profiles generated by ultrasound applicators. The accuracy of the model was verified by comparing the results to published in vivo thermal lesion data. A tumor model was constructed with a 2 x 2 x 2cm^3 tumor volume located 5cm below the body surface. The treatment goal was to deliver to the entire tumor volume a thermal dose higher than 240 EM_{43} while sparing the surrounding tissue by limiting the thermal dose level to less than 60EM43 in regions more than 5 mm beyond the tumor edge. The highly and moderately focused spherical transducers studied here had an identical aperture and operating frequency. The focal length of the moderately focused spherical transducer was chosen so that the number of thermal lesions required for this transducer to treat the tumor was minimized. It was demonstrated that the moderately focused spherical transducer required a total time of 40 min to treat the 2 x 2 *x* 2 cm^3 tumor, while the highly focused spherical transducer required 150 min. However, it was also found that the moderately focused transducer produced more sub-lethal thermal dose in the intervening tissue regions. For example, the $30EM_{43}$ thermal dose contour extended to approximately 1.5cm in front of the target, compared to lcm in the case of the highly focused spherical transducer.

1-Introduction

High intensity focused ultrasound [HIFU] thermal therapy involves raising the temperature of a pre-selected tissue volume to between 50°C and 90°C. The high temperature causes rapid coagulation of the target tissue. Moreover, large thermal gradients in the target region are desired so that the surrounding normal tissue is spared. treatment protocols adopting highly focused transducers were successful
in achieving this goal. However, such protocols were problematic for the treatment of large tissue volumes. Due to the small thermal lesion volume produced for each individual exposure, a large number of ultrasound exposures was required for the complete destruction of the target volume [81]. Moreover, when the transducer was moved to deliver the exposures, some normal tissue in the near field remained in the overlapping beam pathways, as illustrated in figure (1). Although the temperature rise in the near field after a single exposure was low compared to that in the focal region, continua1 exposures of the same tissue region in the near field could result in a large temperature rise and significant thermal damage [2]. Damianou and Hynynen [1] have demonstrated that a cooling period must be employed between exposures to allow tissues in the near field to cool. Consequently, the treatment time for large tissue volumes were impractically long. For example, a study of HIFU thermal treatment by Yang et al. [3] found that 4 hours were required for a highly focused transducer to destroy an 1 cm3 tissue volume in rabbit liver. One approach to reducing the treatment time is to enlarge individual thermal lesions so that their number can be reduced. This can be achieved by increasing exposure duration and/or exposure intensity. However, blood Bow cooling effects associated with long exposures and non-linear ultrasound beam propagation associated with high intensities may make the control of lesion formation difficult. Enlarging thermal lesions can

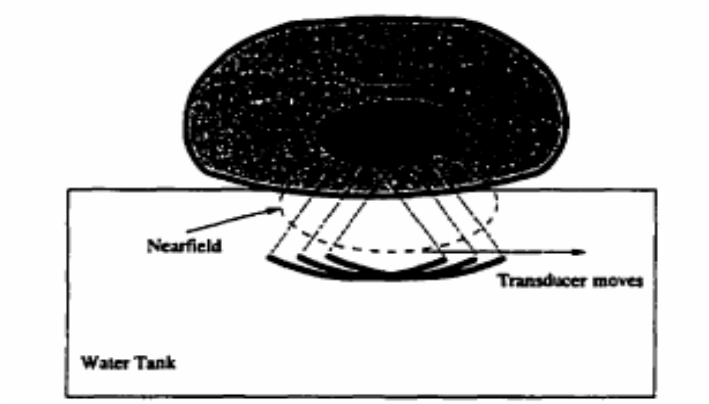

Fig.1. During the transducer movement from left to right to form lesions side by side, some normal tissues in the near field remain in the pathway of the beam.

also be achieved by employing a transducer with a larger focal zone such as the moderately focused spherical transducer. However, the large focal zone associated with the weak focusing results in more heat being delivered to tissues surrounding the target. Due to this safety issue, only one system among al1 the reported HIFU heating systems has employed a moderately focused spherical transducer [4]. Applying this heating system to a phase 1 clinical study, et al. [4] reported encouraging results that the treatment of a 1.3cm3 volume of tumor tissue in kidney required approximately 30-35 min. This result appear to be a significant improvement on the treatment times required with highly focused spherical transducers. However, the conclusion should be drawn with caution as many treatment parameter, including the shape and location of the target volume and the criterion for determining cooling periods, are different between the experimental studies using the highly focused transducer designs and those using the moderately focused spherical transducer designs. A second approach to increasing the volume of individual thermal lesions is through the use of a phased array. Fan and Hygne [5] have developed phased 2-D array ultrasound applicators to generate large thermal lesions, where the focal zone volume was significantly enlarged compared to those of single-focus ultrasound applicators. Daum et al. reported that an approximately 3 cm3 volume of tissue could be thermally destroyed in a single 20s exposure by a 256 element phased 2-D array using a 16 focus field. Compared to phased array designs, moderately focused spherical transducer are simple to construct, inexpensive and commercially available. In addition, unlike the 256 element phased array which required long exposures (20s) to ensure that tissue volumes were completely destroyed by multiple foci, moderately focused spherical transducers, which generate single foci, can adopt short exposures, making lesion formation less dependent on blood flow cooling effects. To quantitatively evaluate the use of moderately focused spherical transducers, a theoretical study is presented here to compare treatment times required for a highly and a moderately focused spherical transducer to treat a 2 x 2 x 2cm^3 tumor volume under identical treatment conditions. An ultrasound-thermal mode1 was developed and used to predict treatment times. Thermal dose profiles generated by these two transducers were also compared to examine the effect of transducer focusing on thermal damage produced in the surrounding tissues.

2- Methods

Ultrasound-Thermal Model

A three dimensional mathematical model was developed to predict ultrasound induced thermal damage in tissues. The model consists of three parts (see figure(2)).

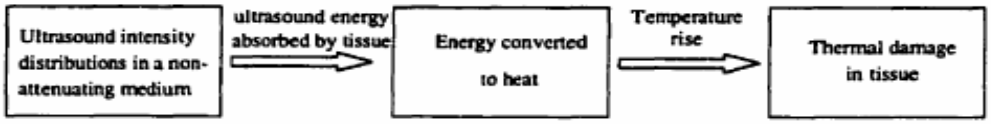

Fig.2.Block diagram of numerical model to simulate ultrasound-thermal effects in tissue.

Ultrasound Intensity Distributions

The first modeling step was to calculate the ultrasound intensity distribution generated by a transducer in a non-attenuating medium. The transducer surface was assumed to be composed of an array of small element sources of ultrasound energy. The contributions from these sources to the intensity at each point in the field were superimposed, according to the Rayleigh-Sommerfeld integral [6].

$$I(x,y,z)=\frac{1}{2\rho c}\left|jk_{wave}c\rho u\iint_{s}\frac{e^{-jk_{wave}d(x,y,z,x_0,y_0,z_0)}}{2\pi d(x,y,z,x_0,y_0,z_0)}ds\right|^2 \quad (1)$$

Where

I =Intensity at the field point (x,y,z)[W.cm^{-2}].
U =particle velocity amplitude at the transducer Surface [cm.s^{-1}].
K_{wave}=wave number[cm^{-1}].
C =speed of sound in medium [cm.s^{-1}].
ρ = density of the medium [g.cm^{-3}].
d =distance [cm] between the source element (x_0,y_0,z_0) and the field point (x,y,z).
ds =surface area of the source element[cm^2].

Heat transfer in tissue

The temperature rise in tissue due to ultrasound exposures was predicted by the Bioheat 'transfer Equation [BHTE] [7]

$$\frac{\partial T(x,y,z,t)}{\partial t}\rho_t c_t+\omega_b c_b\left(T(x,y,z,t)-T_a\right)=k\nabla^2 T(x,y,z,t)+SAR(x,y,z) \quad (2)$$

Where

T = temperature at the field point (x,y,z)at time t[s]
ρ_t = density of tissue [g-cm^{-2}]
C_t = heat capacity of tissue [j.g^{-1}.c^{-1}]
ω_b = volumetric perfusion rate [g.s^{-1} .cm^{-3}]
C_b = heat capacity of arterial blood [j.g^{-1}.c^{1}]
T_s = temperature of arterial blood [C]
K = thermal conductivity of tissue [W.cm^{1}.c^{-1}].
SAR= specific absorption rate [w.cm^{-3}],which is the amount power absorbed by tissue per unit volume.

In this equation, it was assumed that heat transfer between blood vessels and tissues occurred mainly across the microvasculature. The blood in the capillary bed would instantly thermally equilibrate to the temperature of the surrounding tissues. Heat transfer by large vessels which create significant temperature gradients in their vicinity was not taken into account in this model.

The SAR was calculated using equation (3). To simplify the calculations, it was assumed that the attenuated energy can be calculated by integrating the attenuation coefficient over the axial distance traversed.

$$SAR(x,y,z)=I(x,y,z)\cdot e^{-2\mu s(x,y,z)}2\alpha \quad (3)$$

Where

P = amplitude attenuation coefficient [Np. cm^{1}.MHz^{-1} **,**1NP x 8.686 = ldB]
s = axial distance [cm] between the skin surface and the field point (x,y,z).
α = amplitude absorption coefficient

A finite difference algorithm was used to solve the BHTE in Cartesian coordinates[8]. The temperature change was calculated at every node in a computation domain, Temperatures at the boundaries of this computation domain were set to be constant at 37°C. The initial temperature at each node was assumed to be 37°C. To simplify the calculations, al1 tissues within the computation domain were assumed to possess identical acoustic and thermal properties which remained constant during heating.

Thermal damage in tissue

Thermal dose to the tissue was quantified using the following equation [9].

$$TD(x,y,z,t)=\int_{t=0}^{t=t_{total}}R^{T(x,y,z,t)-43}dt\ ,\ R=\begin{cases}2 & T\geq 43^{\circ}C\\ 4 & T<43^{\circ}C\end{cases} \quad (3)$$

Where

TD = thermal dose [EM_{43}]
T_{total}= total treatment time [s]
t = time[s]

This formula has been verified for temperatures up to 57°C [3] and bas been successfully used in predicting thermal lesion size in vivo .

Tumor model

In order to evaluate different transducer geometries in terms of treatment time under identical treatment conditions, a tumor mode1 was developed which included the tumor geometry, tissue properties,

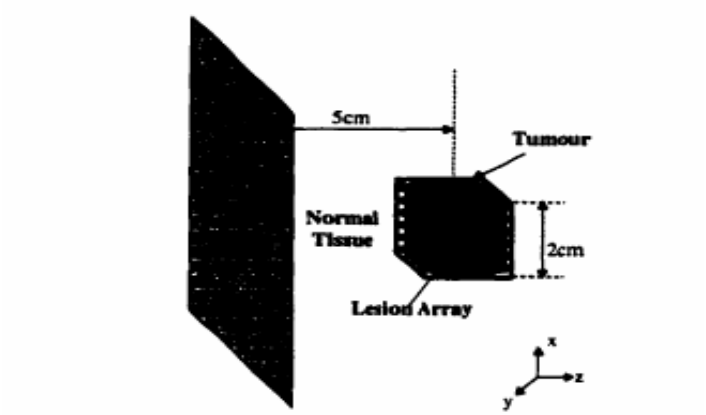

Fig.3. Tumor geometry employed in this work.

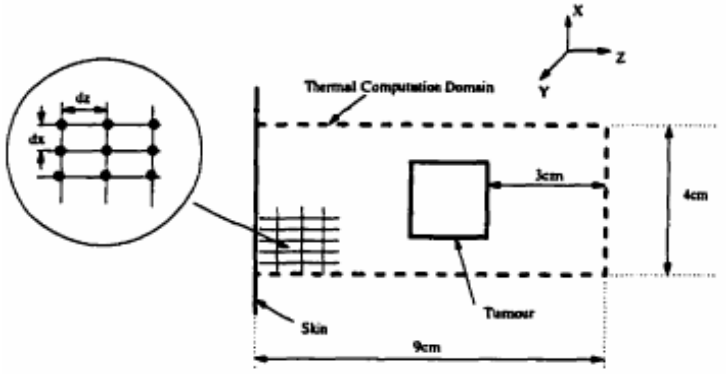

Fig. 4. Thermal computation domain and mesh spacing dx, dy and dz.

thermal dose targets for the tumor and thermal dose limits for the protection of the normal tissue.

The tumor geometry employed in this work is illustrated in figure (3). The tumor selected was in the shape of a cube (2 x 2 x 2cm^3), with its centre located 5cm below the skin surface. A cube shaped target was useful as a first approach in this theoretical investigation because the volume can be easily filled by any array of individual, identical lesions, as illustrated in figure 2.3. Given this tumor size, the size of the thermal computation domain was chosen to be 4 x 4 x 9cm^3, to achieve reasonable computation times (figure (4)). The mesh spacing dx, dy and dz were chosen to be 0.5, 0.5 and 1 mm (figure (4)). The time step was chosen to be 0. 1 S. These were the smallest achievable values given a practical computation time.

Tissue Properties

The values of acoustic and thermal properties of human muscle tissue were used in this study (table (1)). Muscle tissue has a lower perfusion rate than most other tissues, and therefore represents a "worst case" scenario because the near field heating would be large.

atten. coeff. [Np cm^{-1} MHz^{-1}]	.06
absor. coeff. [Np cm^{-1} MHZ^{-1}]	.06
Speed of sound [cm s^{-1}]	1500x10^2
Tissue density [g.cm^{-3}]	1.05
Blood density [g cm^{-3}]	1.06
Tissue heat capacity [J . g^{-1} .C^{-1}]	3.72
Blood heat capacity [J g^{-1} C^{-1}]	3.84
Tissue conductivity [W cm^{-1} C^{-1}]	.005
Perfusion rate [g .s^{-1} cm^{-3}]	.0006

Table .1 .The acoustic and thermal parameters used in this study. These values are taken from Duck [10]. The value of the absorption coefficient is chosen to be the same as that of the attenuation coefficient, in order to simplify the model.

Thermal Dose Thresholds

A thermal lesion was defined as the volume bounded by the 240 EM_{43} thermal dose isosurface. The thermal dose of 240 EM_{43} was selected because it lead to complete

necrosis in a variety of tissues. The cooling time was chosen such that the 60 End_{43} thermal dose contour just extended to 5 mm beyond the tumor boundary (figure (5)). Therefore, the normal tissue 5 mm beyond the tumor boundary would receive a

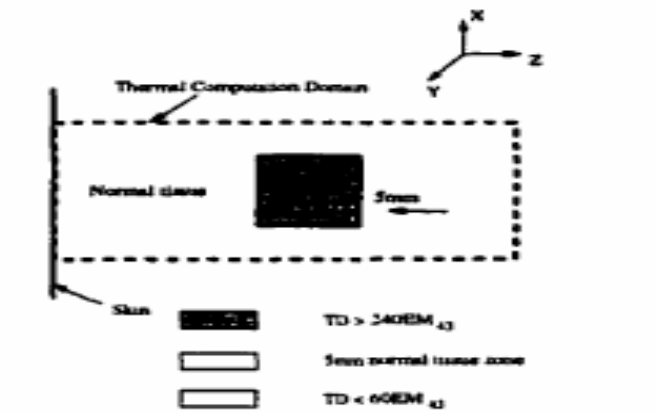

Fig..5. Thermal doses to all of the tumor tissue were intended to be higher than 240 EM_{43} and thermal doses to all of the normal tissue 5 mm beyond the tumor boundary were intended to be lower than 60 EM_{43}.

thermal dose of less than 60 EM_{43}. This was to spare the normal tissue. The value of 60 EM_{43} was selected because a thermal dose of less than 60 EM_{43} would not result in severe damage in most critical tissues and organs (151. The 5 mm normal tissue zone (figure (5)) allowed the 240 EM_{43} thermal dose isosurface to completely encompass the tumor volume by sacrificing some normal tissue directly adjacent to the tumor boundary.

Cooling periods were determined iteratively by simulating entire multi-exposure treatments using the ultrasound-thermal model. After each simulation, the calculated 60 EM_{43} thermal dose contour, based on an initially selected cooling time, was compared with the specified 5mm limit. The cooling time was then adjusted and the simulation repeated as required until the thermal dose limits shown in (figure (5)) were achieved. The cooling time in the first iteration was chosen such that tissues everywhere could cool to $43^{O}C$ before the next exposure was delivered.

3- Results

Verification of Ultrasound-Thermal Mode1 Accuracy

The accuracy of the mathematical model was determined by comparing predicted transducer 6dB beam lengths , bandwidths and thermal lesion dimensions with published experimental data.

Applicator used by	Sanghvi et al. [59]	Watkin et al. [79]	Chen et al. [7]
Focal length (cm) Diameter (cm) Operating frequency (MHz)	7.5 5.5 4	15 10 1.68	14 10 1.7
6dB beam length measured (mm) :predicted (mm) (% difference)	7:6.6 -5%	19:18.5 -2%	18:16.2 -10%
6dB beam width measured (mm) :predicted (mm) (% difference)	.65:.75 15%	1.7:1.9 12%	1.6:1.8 12.5%

Table. 2. Measured and predicted 6dB beam length and beam width of the applicators used by Sanghvi *et* al. [14], Chen *et al.* [12] and Watkin et al. [13]. The % difference between the measured and predicted values was calculated as((predicted-measured)/measured).

Verifying Intensity Distribution Predictions

Intensity distribution calculations for transducers in a non-attenuating medium were verified by comparing predicted beam lengths and beam widths to the published experimental data of three applicators table(2). Two of these applicators, used by Sanghvi et al. [14] and Watkin et al. [13], consisted of single spherical shaped transducers. The third applicator, used by Chen et al. [12], was a combination of a

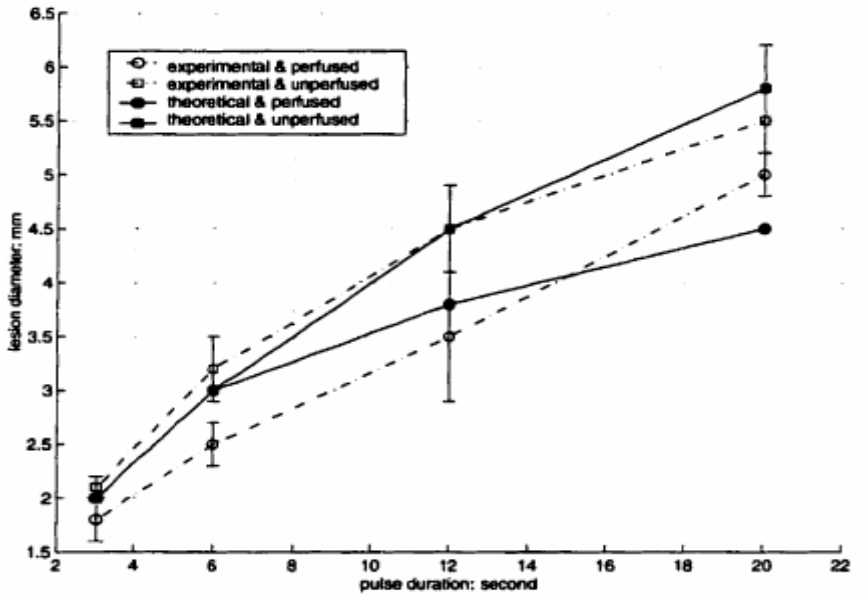

Fig. 6. Comparison of measured lesion diameters with the results predicted by our theoretical model.

planar transducer and a converging lens. The results indicate that the theoretical model overestimated the 6dB beam width for all three transducers. The largest difference (15%) occurred for the highly focused transducer of Sanghvi et al. [14].

The difference reduced to 12% for the moderately focused transducer of Watkin et al. [13]. The model underestimated the 6dB beam length by 5% for the highly focused transducer of Sanghvi et al. [14] and 2% for the moderately focused transducer of Watkin et al. [13]. The large difference of 10% between the measured and predicted -6dB beamlengths for the lens/transducer combination was probably caused by the spherical aberration of the lens.

Verifying Thermal Dose Predictions

Thermal dose calculations were tested by comparing the predicted lesion size with experimentally measured data [12]. Cases with and without blood flow were tested. In Chen et al. [12], thermal lesions were consistently formed 2 mm below the surface of rat liver using the focused spherical applicator described above. During these experiments, the rat liver was exposed so that the liver could be accessed directly with the ultrasound beam without passing through intervening tissue layers. In the theoretical predictions, tissue acoustic and thermal properties were chosen to match the experimental conditions table(.3). The volume bounded by the thermal dose isosurface of 30 EM_{43} (as opposed to the 240 EM_{43} used in subsequent investigations) was defined here as the thermal lesion volume. The thermal dose of $30EM_{43}$ was found to induce heptocyte loss and fibrosis in dog liver tissue[15].

atten. Coeff	.078
absor. coeff.	.037
Speed of sound	$1550x10^2$
Tissue density	1.05
Blood density	1.06
Tissue heat capacity	3.6
Blood heat capacity	3.84
Tissue conductivity	.005
Perfusion rate	.04 or0

Table.3.Tissue acoustic and thermal properties used in prediction of lesion size in rat liver .

Figure (6) compares the measured and predicted lesion diameters. The theoretical values of lesion diameter were measured from the calculated thermal dose profiles, as illustrated in figure (7).

In most cases, the predicted thermal lesion dimensions fell within the experimental error range, and agreement was better for the non-perfused cases. For the perfused cases, the mode1 overestimated lesion diameters by approximately 12% for short exposures of 3s and 6s and underestimated lesion diameters by 10% for the long exposure of 20 S. A possible explanation of the overestimation for 3 s and 6s exposure cases was that the perfusion rate used in the theoretical predictions was lower than that in the experimental situation. For the case of 20s exposure, micro-

vasculature collapse is expected to occur during heating [go], which would have reduced the perfusion cooling effect and allowed for a larger lesion volume. In our model, however, the perfusion rate was assumed to be constant regardless of heating

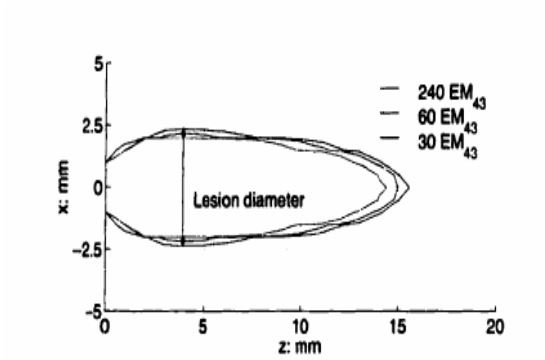

Fig. 7. Thermal dose distributions calculated using our theoretical model. Treatment parameters, tissue acoustic and thermal properties were chosen to math the experimental conditions (table 3). The non-perfused, 12 s heating exposure case was shown here.

Comparison of Highly and Moderately Focused Spherical Transducers

Physical parameters of the highly focused (denoted as SPI) and the moderately focused (denoted as SP2) spherical transducer investigated in this study are given in table (4)**.** Exposures of 10 s were adopted for both designs, which are sufficiently brief to limit the blood flow cooling effects in the case of low perfused tissues [16l], but also long enough to allow relatively large thermal lesions to be produced. SP2 had the same aperture and operating frequency as SPI, but a larger radius of curvature. The radius of curvature of SP2 was selected such that the thermal lesion generated by it in a 10s exposure would be slightly larger in the axial direction than the tumors.

The determination of the radius of curvature of SP2 was based on figure (8), which shows lesion length and diameter after a 10 s exposure versus radius of curvature of focused spherical transducers. The thermal lesions were placed at the centre of the tumor. Spatial peak intensities [17] were chosen such that the predicted maximum temperature in the tissue after the exposure [T_{peak}] was approximately $85^{O}C$ to avoid tissue vaporization. The values of I_{SP} are given in table (5).

	SP1	SP2
Radius of curvature (cm)	8.5	13
Aperture (cm)	10	10
Operating frequency(MHz)	1	1
Beam width (mm)	1.9	3
Beam length (mm)	10	23

Table. 4. Physical parameters of two focused spherical transducers studied in this work.

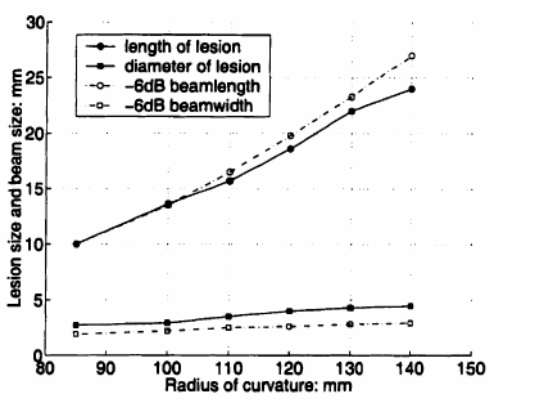

Fig .8.Lesion length and diameter and transducer 6dB beam length and beam width versus radius of curvature of focused spherical transducers. The transducers were assumed to give a 10 s exposure to the tumor.

Focal length (cm)	$T_{peak}(^{O}C)$	I_{SP} (W cm^{-2})	Acoustic power output (W)
8.5	85.1	1003	14.4
10	85.6	900	16.8
11	85.4	803	21.2
12	85.9	740	21.4
13	85.9	683	22.5
14	85.7	619	

Table.5. Spatial peak intensities used in figure.8.

The relative intensity distributions of SPI and SP2 and thermal doses generated by these two transducers For a single 10 s exposure are plotted in figure (9). Both these transducer produced single, ellipsoid-shaped focal zones and similarly.

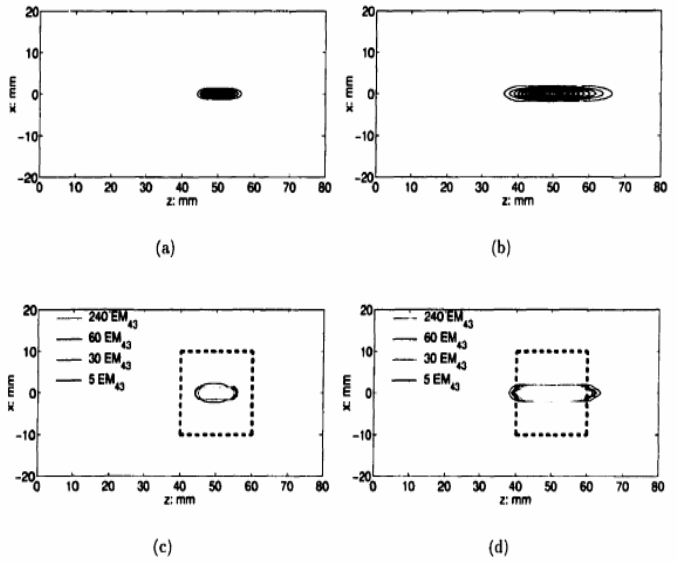

Fig.9. Figures (a) and (b) show relative ultrasound intensity distributions produced by SP1 and SP2 respectively. The distributions are shown as contour plots relative to the peak value in 10% intervals starting at 10%. The axial planes at y=0 mrn are displayed. The focal plane is at z=50mm. Figures (c) and (d) show the thermal dose profiles generated by SPI and SP2 respectively. The thermal dose profiles are displayed as contour plots, showing contours representing 240, 60, 30 and 5 EM_{43}, progressing outwards from the lesion centre. Dashed lines represent the tumor boundary. The lesions were produced by placing the centre of the focal zone at the centre of the tumor and delivering a 10 s exposure

shaped thermal lesions (the volume bounded by the 240 EM_{43} thermal dose contour). Figure (9-a) and (9-b) show that intensity gradients generated by SP2 are smaller than those generated by SPI. Figure (9 -c) and (9-d) show that both SPI and SP2 produced sharp thermal dose gradients over a single exposure. The distance between the 240 EM_{43} and 5 EM_{43} contours in the axial direction for SPI was slightly shorter than that for SP2.

Since the length of the thermal lesion generated by SPI was only 50% of the tumor length (z direction), two lesions arrays at two different depths, separated by 10 mm, were required for the treatment. Only one lesion array was required for SP2 because the size of thermal lesions was equal to the size of the tumor along the z direction. Moreover, more thermal lesions were required to cover al1 of the tumor in the lateral direction for SPI because individual lesions were smaller in diameter compared to those generated by SP2.

Figure (10) illustrates transducer step patterns employed for SPI and SP2. Axial movement of SPI focus was chosen to step from the distal region of the tumor towards the proximal region (figure 10-a)). This pattern was chosen to avoid coagulated tissue being present in the pre-focal regions of subsequent exposures. Coagulated tissue, which attenuates ultrasound more than un coagulated tissue [18], [19], would prevent penetration of ultrasound fields to distal regions. The lateral step patterns (figure 2.10 (b) and (c)) were suggested by Fan and Hynynen (1996). The advantage of these patterns was that excessive heating was avoided by delivering successive exposures to regions which were not adjacent to each other. After determination of the transducer step patterns, treatments were simulated to determine the cooling times required to spare the surrounding normal tissue. Table (6) compares the number of exposures, exposure times, cooling times and total treatment times required for SP1 and SP2 to treat the tumor. The maximum tissue temperatures predicted are also given in table(6). They are higher than the T_{peak} in single exposures, because of the heat accumulation, but lower than the vaporization temperature of 100°C.

Temperatures reached in the tissue during the entire treatment using SP2 were shown in figure (11). Figure (1 1) shows that immediately after the first heating exposure, which was given to the center of the tumor, the tissue temperature at (0, 0, 4 cm) reached the maximum value. The temperature then dropped during the cooling period. As the transducer moved to heat the peripheral region of the tumor, the peak temperatures at (0, 0, 4cm) after individual exposures gradually decreased, because little

amount of energy was deposited at this location. The gradua1 increase in temperature at (0, 0, 3.5cm) and (0,0, 1 cm) during the initial 15 exposures indicates that heat accumulates at these locations. The highest tissue temperature ever reached during the treatment at 1cm below the skin surface was approximately 41^0C.

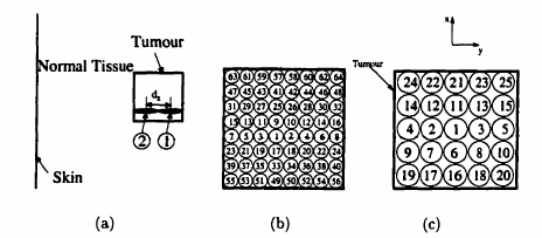

Fig.10. Transducer step patterns for SPI ((a) axial and (b) lateral) and SP2 *((c)* lateral).

	SP1	SP2
Number of exposures	128	25
Exposure time [s]	10	10
Spatial peak intensity [W.cm^{-2}]	1003	683
Acoustic power output [W]	14.4	22.4
Maximum temperature [^{o}C]	88	90
Total time [hour]	60	90
	2.5	.7

Table. 6. Total treatment times, number of exposures, exposure times and intensities, and cooling times for SP1 and SP2 to treat the tumor. The acoustic power outputs over each exposure and the maximum temperatures occurred in the tissue during multiple exposures are also listed.

Thermal dose profiles produced at the end of the treatments using SPI and SP2 are displayed in figure (12). Figure (12) shows that in both treatments, some small volumes of tumor tissue received a sub-lethal thermal dose of less than 240 EM_{43}. This could have been avoided if more lesions had been formed. Comparison of figure (12-a) and figure (12-c) indicates that, at the end of the treatments, the thermal dose delivered to the near field by SP2 was greater than for SPI. For comparison, thermal dose profiles generated by SPI and SP2 with longer cooling times are displayed in figure (13), where the cooling times were chosen such that the 30 EM_{43} thermal dose contour extended approximately 5 mm beyond the tumor boundary at the end of the treatment (as opposed to the 60 EM_{43} threshold used in figure 2.12). Given this criterion, the cooling periods chosen were 70s and 120 **s** for SPI and SP2 respectively. The resulting total treatment times were 2.8 hour and 0.9 hour for SPI and SP2 respectively. Comparison of figure (12-c) and figure (13-c) shows t hat the thermal dose delivered to the near field **was** significantly reduced due to the longer cooling period**.**

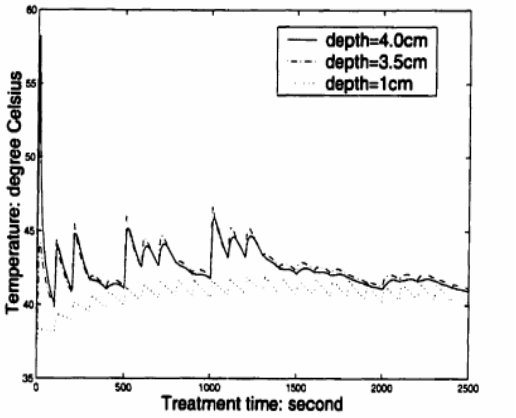

Fig 11. Temperatures reached in the tissue as a function of time during the tumor treatment using SP2. Temperatures of the tissue that was located on the central axis (x=O mm, y=O mm) were plotted.

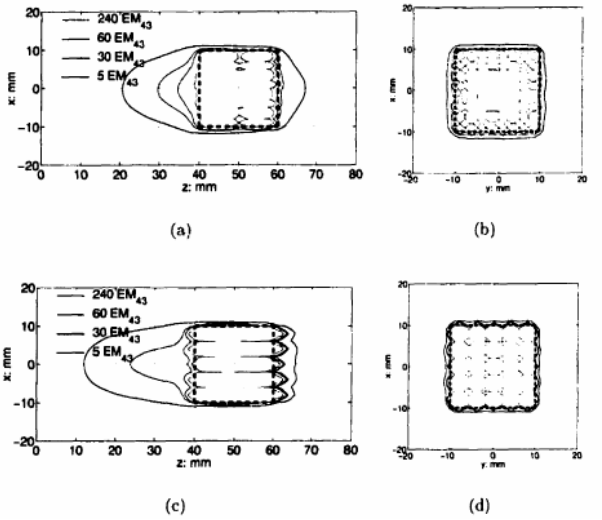

Fig.12.Thermal dose profiles for treatments of the tumor using SPI (a, b) and SP? (c,d). The cooling time in the treatments was chosen such that the *60* EM_{43} thermal dose contour just extended to 5mni beyond the turn our boundary at the end of the treatments. Figures (a), (c) show the axial plane y=0 mm, where the 5, 30 a d 60E& thermal dose contours are maximally extended beyond the tumor boundary. Figures (b), (d) show the lateral plane z=50 mm. Thermal dose profiles are displayed as contour plots, representing 240, 60, 30 =and 5 EM_{43} Dashed lines represent the tumor boundary.

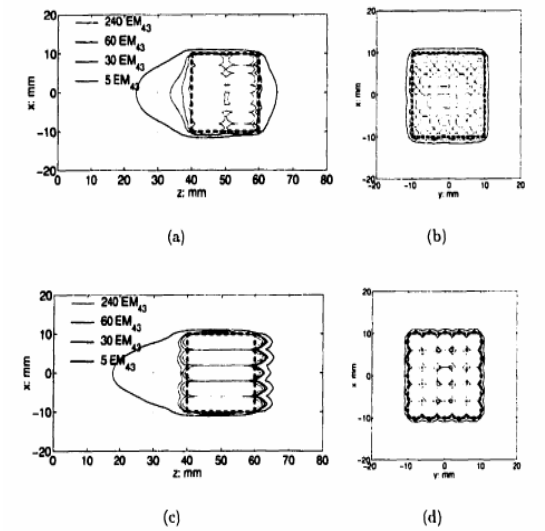

Fig.13: Thermal dose distributions for treatments of the tumor using SPI (a, b) and SP2 (c,d). The cooling time in the treatments was chosen such that the 30 EM_{43} thermal dose contour just extended to 5mm beyond the tumor boundary at the end of the treatments. Figures (a), *(c)* show the axial plane y=0 mm, where the 5, 30 and 60EM_{43} thermal dose contours are maximally extended beyond the tumor boundary. Figures (b), (d) show the lateral plane z=50 mn. Thermal dose profiles are displayed as contour plots, representing 240, 60, 30 and 5 EM_{43}. Dashed lines represent the tumor boundary.

4-Discussion

The results showed that for the treatment of a 2 x 2 **x** 2 cm3 tumor 5 cm deep in the body, the moderately focused spherical transducer required 42 min, 28% of the time required for the highly focused spherical transducer . This demonstrates a significant improvement in total treatment time by the use of the moderately focused spherical transducer. Although the comparison was performed under identical treatment conditions, this conclusion should still be drawn with caution. Firstly, if the criterion for choosing cooling periods is changed, the difference between treatment times required by the highly and moderately focused spherical transducers may also change. For example, when the 30 EM_{43} thermal dose contour extending no further than 5 mm beyond the tumor boundary was employed as the normal tissue thermal dose limit, the moderately focused spherical transducer required 54 min to treat the same tumor volume. This indicates that **as** the thermal sensitivity of the normal tissues surrounding the target increases, the ability of moderately focused spherical transducer to reduce the treatment time maybe reduced, due to the increase in cooling period required. Secondly, the ability of moderately focused spherical transducers to reduce the treatment time also depends on the shape of the target. Figure (8) indicates that thermal lesions generated by moderately focused spherical transducers over single exposures are elongated. Thus, the use of moderately focused spherical transducers enlarges thermal lesions mainly in the axial direction compared to the use of highly focused spherical transducers. Hence, for the treatment of tumor volumes which are small in the axial direction, moderately focused spherical transducers will not offer any improvement in treatment time. On the other hand, the use of moderately focused spherical transducers will be more effective in reducing treatment time if the axial dimension of the tumor volume is larger than that investigated here.

To simplify the calculations and reduce computation time, constant tissue ultrasound attenuation and constant perfusion were assumed in the ultrasound thermal model. Tissue ultrasound attenuation, however, has been demonstrated to increase with temperature and time during heating [13,26]. In addition, perfusion has been found to decrease with increasing temperature and time [20**].** The assumption of constant perfusion may lead to an underestimation of the thermal lesion Volume . Since a relatively low perfusion rate was assumed in this study, the assumption of constant perfusion was expected to have a small effect on treatment time comparison result. A preliminary study conducted by Kolios [21] has demonstrated that the assumption of constant ultrasound attenuation resulted in an overestimation of the axial dimension of the thermal lesion volume and an underestimation of the lateral dimension of the thermal lesion volume. However, the effect of the assumption of constant ultrasound attenuation on treatment time calculation result is not known.

5-Conclusions

This study also examined the effects of the weak focusing on treatment outcomes including thermal dose profiles and the selection of cooling periods. To limit the thermal dose to the surrounding tissue below the threshold, the moderately focused spherical transducer required a cooling period of 90 s between exposures, as compared to 60s for the highly focused spherical transducer. Although the difference between thermal dose gradients generated by the highly and moderately focused spherical transducers is small over single exposures, it increases over multiple exposures in the near field region, due to heat accumulation. This indicates that the use of a moderately focused transducer will lead to more (sub-lethal) thermal dose deposited in the intervening tissue regions.

In order to further reduce the number of thermal lesions to make treatments of large tissue volumes

more efficient, transducer designs capable of producing thermal lesions larger in the lateral dimension must be employed. Phased 2-D arrays [22] and multi-focus acoustic lens/transducer combinations [23], which are capable of generating multiple focus fields, are potential solutions.

A 3-D mathematical model was developed to predict ultrasound-induced thermal damage in tissue. The accuracy of the model was verified by comparing the predicted results with published in vivo lesion data. The predicted thermal lesion size agreed with measured results [23] for the non-perfuse cases. For the case of high perfusion rates, the difference between measured and predicted lesion sizes was attributed to a difference between the perfusion rate in the experimental conditions and the value used in simulations and to changes in perfusion during heating that were not modeled. By using the ultrasound-thermal model, treatments of a 2 x 2 x 2cm3 tumor volume using a highly and a moderately focused spherical transducer were simulated, and the total treatment times were determined. It was demonstrated that the moderately focused spherical transducer required a total time of 42 min to treat the tumor, 28% of the time required by the highly focused spherical traducer. However, the use of the moderately focused spherical transducer resulted in more (sub-lethal) thermal dose being delivered to the intervening tissue regions. The study suggests that transducer designs capable of generating larger thermal lesions should be employed to further reduce the total treatment time for large tissue volumes.

6- References

[1] C. Damianou and K. Hynynen. Focal spacing and near-field heating during pulsed high temperature ultrasound therapy. Ultrasound *in* Medicine and Biology, 19(9) : 777-787, 1993.

[2] K. Hynynen, A. Darkazanli, E. Unger, and J. F. Schenck. Mri-guided noninvasive ultrasound surgery. Medical Physics, 20: 107-1 15, 1993.

[3] R. Yang, N. T. Sanghvi, 3. R. Rederick, C. A. Galliani, F. J. Fry, S. L. Griffith, and J . L. Grosfeld. Extracorporeal liver ablation using sonography-guided high intensity focused ultrasound. Investigative Radiology, 27:796-803, 1992.

[4] A. Visioli, 1. H. Rivens, Gai1 ter Haar, A. Horwich, R. Huddart, E. Moskovic, A. Padhani, and J. Glees. Preliminary results of a phase 1 dose escalation clinical trial using focused ultrasound in the treatment of localized tumors. European Journal of Ultrasound, 9: 11-18, 1999.

[5] X. Fan and K. Hynynen. A study of various parameters of spherically curved phased arrays for noninvasive ultrasound surgery. Physics in Medicine and Biology, 41 (4):591-608, April 1996.

[6] H.T. O'Neil. Theory of focusing radiators. Journal of the Acoustical Society of America, 21516-526, 1949.

[7] H. H. Pennes. Analysis of tissue and arterial blood temperatures in the resting human forearm. Journal of Applied Physiology, 1:93-122, 1948.

[8] M. C. Kolios, M. D. Sherar, **A. E.** Worthington, and J. W. Hunt. Modeling temperature gradients near large vessels in perfused tissues. In M. A. Ebadian and P. H. Oosthuizen, editors, Fundamentals of Biomedical Heat Transfer, pp 23-30, HTD-Vo1.295, 1994.

[9] S. A. Sapareto and W. C. Dewey. Thermal dose determination in cancer therapy. International Journal of Radiation Oncology, Biology and Physics, 10:787- 800, 1984.

[10] J**.** Borrelli, L. L. Thompson, C. C. Cain, and W. C. Dewey. Time-temperature analysis of ce11 killing of BHK cells heated at temperatures in the range of 43.5 C to 57.0 C. International Journal of Radiation Oncology, Biology and Physics, 19:389-399, 1990.

[11] C. A. Damianou, K. Hynynen, and X. Fan. Evaluation of accuracy of a theoretical mode1 for predicting the necrosed tissue volume during focused ultrasound surgery. IEEE Transactions on Ultrasonic, Ferroelectrics and Frequency Control, 42(2):182-187, 1995.

[12] F. A. Duck. Physical Properties of Tissues: A Comprehensive Reference Book. Academic Press, San Diego, 1990.

[13] N. A. Watkin, G. A. ter Haar, and I. Rivens. High-intensity focused ultrasound ablation of the kidney in a large animal model. Journal of End urology, 11 (3): 191-196, 1997.

[14] N. T. Sanghvi, F. J. Fry, R. Bihrle, R. S. Foster, M. H. Pliillips, J Syrus, A. V. Zaitsev, and C. W. Hennige. Noninvasive surgery of prostate tissue by high intensity focused ultrasound. IEEE Transactions on Ultrasonic, Ferroelectrics and Frequency Control, 43(6): 1099-1 1 10, 1996.

[15] W. C. Dewey. Arrhenius relationships from the molecule and ce11 to the clinic. International Journal of Hyperthermia, 10(4):457-483, 1994.

[16] R. Yang, C. R. Reilly, F. J. Rescorla, P. R. Faught, N. T. Sanghvi, F. J. fiy, Tg D. Franklin, L. Lumeng, and J. L. Grosfeld. High intensity focused ultrasound in the treatment of experimental liver cancer. Archives of Surgery, 126:1002-1010,1991.

[17] C. Damianou and K. Hynynen. The effect -.f various physical parameters on the size and shape of necrosed tissue volume during ultrasound surgery. Journal of the Acoustical Society of Arnerica, 95(3): 1641-1649, 1994.

[18] M. R. Gertner, B. C. Wilson, and M. D. Sherar. Ultrasound properties of liver tissue during heating. Ultrasound in Medicine and Biology, 23(9):1395-1403, 1997.

[19] C. A. Damianou, N. T. Sanghvi, F. J. Fry, and R. Maass-Moreno. Dependence of ultrasonic attenuation and absorption in dog soft tissues on temperature and thermal dose. Journal of the Acoustical Society of America, 102(1):628- 634, 1997.

[20] M. C. Kolios. Applications and validation of models of heat transfer in perfused tissues. PhD thesis, University of Toronto, Ph. D. Thesis, 1998.

[21] S. L. Brown, J. W. Hunt, and R. P. Hill. Differential thermal sensitivity of tumor and normal tissue rnicrovascular response during hyperthermia. International Journal of Hyperthermia, 8(4):501-514, 1993.

[22] D. R. Daum and K. Hynynen. A 256-element ultrasonic phased array system for the treatment of large volumes of deep seated tissue. IEEE Transactions on Ultrasonic, Ferroelectrics, and Frequency y Control, 46(5) : 1254-1268, 1999.

[23] L. Chen, ***G.*** ter Haar, C. R. Hill, M. Dworkin, P. Carnochan, H. Young, and J. P.. Bensted. Effect of blood perfusion on the ablation of liver parenchyma with high-intensity focused ultrasound. Physics in Medicine and Biology, 38(11):1661-1673, 1993.